Phys. Status Solidi RRL **6**, No. 3, 123–125 (2012) / **DOI** 10.1002/pssr.201105564

pss +++rapid research letters+++
www.pss-rapid.com

Low-temperature photoluminescence studies of In-rich InAlN nanocolumns

Jumpei Kamimura[*, 1], **Katsumi Kishino**[**, 1, 2], **and Akihiko Kikuchi**[1, 2]

[1] Department of Engineering and Applied Sciences, Sophia University, 7-1 Kioi-cho, Chiyoda-ku, Tokyo 102-8554, Japan
[2] Sophia Nanotechnology Research Center, Sophia University, 7-1 Kioi-cho, Chiyoda-ku, Tokyo 102-8554, Japan

Received 30 November 2011, revised 31 December 2011, accepted 2 January 2012
Published online 9 January 2012

Keywords nanocolumns, nanowires, InAlN, photoluminescence, molecular beam epitaxy

[*] Corresponding author: e-mail kamimura@katsumi.ee.sophia.ac.jp, Phone: +81 3 3238 3323, Fax: +81 3 3238 3321
[**] e-mail kishino@katsumi.ee.sophia.ac.jp, Phone: +81 3 3238 3323, Fax: +81 3 3238 3321

High-quality $In_xAl_{1-x}N$ ($0.71 \le x_{In} \le 1.00$) nanocolumns (NCs) have been grown on Si(111) substrates by rf-plasma-assisted molecular-beam epitaxy (rf-MBE). Low-temperature photoluminescence (LT-PL) spectra of various In-rich InAlN NCs were measured at 4 K and single peak PL emissions were observed in the wavelength region from 0.89 μm to 1.79 μm. Temperature-dependent PL spectra of $In_{0.92}Al_{0.08}N$ NCs were studied and the so-called "S-shape" (decrease–increase–decrease) PL peak energy shift was observed with increasing temperature. This shift indicates the carrier localization induced by the In segregation effect and is different from the anomalous blue shift frequently observed in InN films and nanowires with high residual carrier concentrations.

1 Introduction InAlN alloys are attractive for potential applications to devices such as light emitters and detectors, working in the wide photon energy range from 0.63 eV to 6.2 eV, viz., from infrared to ultraviolet [1–4]. As the lattice parameter of $In_xAl_{1-x}N$ can be matched to that of GaN at $x = 0.15–0.18$, the lattice-matched GaN/InAlN system has been employed for the fabrication of distributed Bragg reflectors (DBRs) [5]. For high-In-composition InAlN, however, few studies have been reported [6–8] and the poor optical quality of the InAlN due to its immiscibility caused almost no photoluminescence [9, 10]. Moreover, the growth of self-organized bottom-up nanocrystals is well known as a method of achieving high-quality crystals with ease [11, 12]. In addition, InAlN tended to grow a columnar structure although the growth was aimed at a film [13, 14]. Therefore, it is reasonable to grow a columnar InAlN nanostructure by design. So far, we have reported the growth of In-rich InAlN nanocolumns (NCs) on Si(111) substrates by rf-MBE [15]. In this Letter, the optical properties of the In-rich InAlN NCs are discussed in detail on the basis of the LT-PL measurements.

2 Experimental section The samples were grown by rf-MBE in the growth temperature range of 370–500 °C under nitrogen-rich condition; the composition of In was controlled by changing the beam supply ratio of In to Al. The details of the growth procedure are described in Ref. [15]. Figure 1(a)–(c) show cross-sectional and top view SEM images of $In_xAl_{1-x}N$ NC samples with different average In contents of (a) 0.92, (b) 0.81, and (c) 0.71. The amount of x_{In} was estimated by X-ray diffraction (XRD) using Vegard's law. The InAlN NCs were grown along the *c*-axis, standing independently, having a diameter of 40–130 nm and a length of 0.7–1.1 μm. The PL spectra of $In_xAl_{1-x}N$ ($0.71 \le x \le 1.00$) NCs were evaluated at 4 K under a cw Nd:YAG laser excitation at 532 nm. In the experiment, a liquid helium cryostat was employed and the signals were collected by off-axis parabolic mirrors focused into a monochromator and detected by a liquid-nitrogen-cooled InGaAs array detector.

3 Results and discussion Figure 2 shows the 4 K PL spectra of the $In_xAl_{1-x}N$ NCs with different In compositions, where the PL peak energies were 0.692 eV (1.79 μm in wavelength) for the $x = 1.00$ sample, 0.954 eV (1.30 μm) for $x = 0.89$, 1.21 eV (1.02 μm) for $x = 0.80$ eV and 1.39 eV (0.892 μm) for $x = 0.71$. The emission of In-rich InAlN NCs covered the wide spectral region in the optical communication wavelength range of 1.3–1.7 μm. The inset of Fig. 2 shows the dependence of LT-PL peak

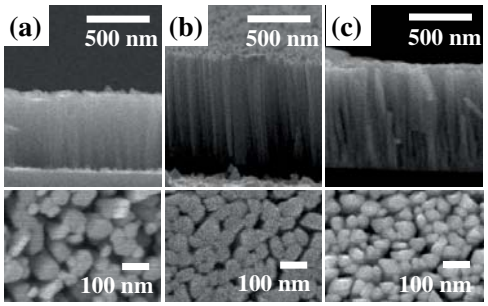

Figure 1 Cross-sectional and top-view SEM images of $In_xAl_{1-x}N$ NCs [(a) $x = 0.92$, (b) $x = 0.81$, and (c) $x = 0.71$].

energy on x_{In}. The peak energies were fitted using the expression

$$E_g(x) = xE_g(\mathrm{InN}) + (1-x)\,E_g(\mathrm{AlN}) - bx(1-x)\,. \qquad (1)$$

Here, we used the low-temperature band gap energy of AlN (6.25 eV) [16]. The best-fitted curve, which is shown in the inset of Fig. 2, was achieved with the bowing parameter b of 4.08 eV. This b value lies between 3.0 [17] and 4.7 eV [18] obtained from the optical absorption data, and is also in good agreement with the first-principles calculations of 3.46–3.67 eV [19] and 4.09 eV [20]. The LT-PL spectral linewidth of InAlN NCs is plotted using open triangles as a function of In composition in Fig. 3, in which the data of InAlN [5, 21–24] and AlN [25] films reported in the literature are also included. The solid curve was obtained from the alloy broadening model [26–29] expressed as

$$\sigma_E = 0.41 \cdot 2\sqrt{2\ln 2}\left|\frac{dE_g}{dx}\right|\sqrt{\frac{x(1-x)}{kV_{exc}}}\,, \qquad (2)$$

where dE_g/dx is the variation of the band gap energy of $In_xAl_{1-x}N$ and $k = 6/(3/2 \cdot 3^{0.5}a_{(x)}{}^2c_{(x)})$ is the cation density in a wurtzite lattice, calculated using the lattice constants $a_{(x)} = 0.3112(1-x) + 0.3545x$ and $c_{(x)} = 0.5703x + 0.4982(1-x)$ [16]. $V_{exc} = (4/3)\,\pi r_B^3$ indicates the exciton volume; the Bohr radius of an exciton r_B is calculated using the dielectric constant $\varepsilon(x) = 8.0x + 6.3(1-x)$, the electron effective mass $m_e/m_0 = 0.085x + 0.48(1-x)$ and the hole effective mass $m_h/m_0 = 0.42x + 3.3(1-x)$, changing from 6 nm in InN to 0.8 nm in AlN. Note that we assume a relatively small dielectric constant and a relatively large effective mass for InN to fit the linewidth of $In_{0.18}Al_{0.82}N$ reported in Ref. [5]. The calculated alloy broadening value is maximized at $x = 0.18$, while the experimental PL-FWHM value decreases monotonically with x. The difference between the calculated and experimental PL-FWHM values is much larger in the x_{In} region lower than 0.18, while a certain discrepancy occurs in the x_{In} region higher than 0.18. Thus, the experimental spectral broadening cannot be explained only by the statistically random alloy disorder, suggesting the existence of an additional inhomogeneity in the In composition, like wire-to-wire and interwire In fluctuation observed in InGaN nanowires [30].

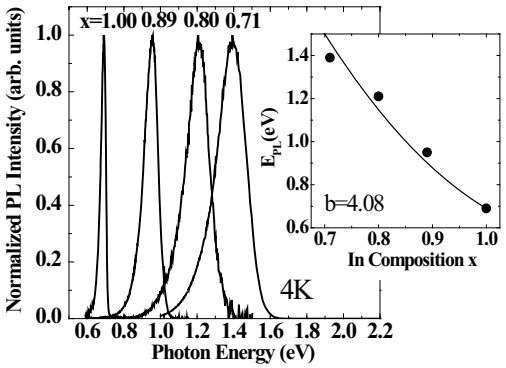

Figure 2 PL spectra of $In_xAl_{1-x}N$ NCs at temperature of 4 K. The inset shows the variation in PL peak energy as a function of In composition x ($0.71 \le x \le 1.00$).

The $In_{0.92}Al_{0.08}N$ NCs were grown at temperatures of 480 °C, 460 °C, and 420 °C under nitrogen-rich condition. A high V/III ratio was applied for high growth temperature to suppress phase separation. The average diameter, length and density of NCs at 480 °C, 460 °C, and 420 °C were (43 nm, 0.9 μm and 2.5×10^9 cm^{-2}), (80 nm, 1.1 μm and 2.7×10^9 cm^{-2}) and (63 nm, 0.7 μm and 6.5×10^9 cm^{-2}), respectively. With increasing growth temperature, the PL peak energy decreased remarkably from 0.972 eV to 0.775 eV and the PL-FWHM at 4 K decreased from 158 meV to 93 meV, although all the three samples had the same In content. The red shift in PL peak energy indicates the decreased residual carrier density and the suppressed Burstein–Moss band filling effect. The narrowing in the PL linewidth observed with increasing growth temperature suggests the suppressed spatial In composition inhomogeneity.

The temperature dependence of the PL spectrum of the $In_{0.92}Al_{0.08}N$ NCs grown at 480 °C was evaluated in the range from 4 K to 300 K, as shown in Fig. 4(a). An "S-shape" PL peak energy shift (decrease–increase–decrease) was observed with increasing temperature; this phenomenon has frequently been reported in Ga-rich InGaN [31], InGaN/GaN quantum wells [32, 33] and In-rich InGaN [34]. It has been explained in terms of band

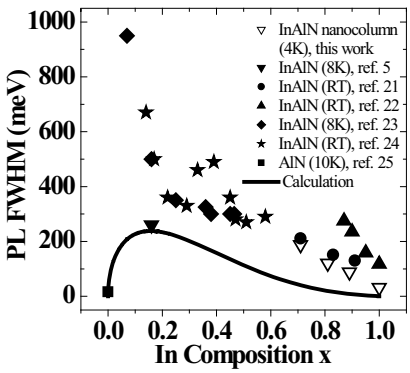

Figure 3 PL FWHM of $In_xAl_{1-x}N$ NCs as a function of In composition x ($0.71 \le x \le 1.00$). This figure includes the AlN and InAlN film data reported by other groups.

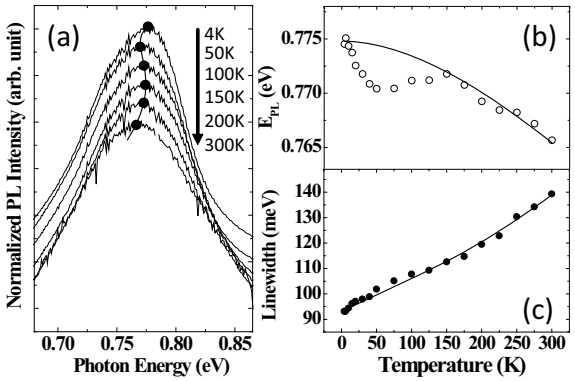

Figure 4 (a) Temperature dependence of PL spectra, (b) peak energy, and (c) linewidth of $In_{0.92}Al_{0.08}N$ NCs grown at 480 °C.

gap shrinkage due to lattice dilation and carrier recombination dynamics using the model of band-edge carrier localization caused by In compositional fluctuation. The PL peak energy versus temperature plot is shown in Fig. 4(b), where the solid line indicates the curve of the PL peak energy calculated using Varshni's equation [35]:

$$E_{PL}(T) = E_{PL}(0) - \frac{\alpha T^2}{T+\beta}, \tag{3}$$

where $E_{PL}(0) = 0.775$ eV, $\alpha = 0.09$ meV/K, and $\beta = 535$, which are linearly interpolated between those of InN [36] and AlN [16]. Note that the PL peak energy shifted basically toward the low energy side (red shift) from 0.775 eV to 0.766 eV, having a small S-shape shift with increasing temperature, contrary to the anomalous blue shift often observed in InN films [3] and nanowires [37], which was caused by high residual carrier density ($>6 \times 10^{18}$ cm^{-3}) [38].

The linewidth of the PL spectrum increased monotonically with respect to the temperature [see Fig. 4(c)], similarly to that observed in the case of an InGaN single quantum well (SQW) emitting violet/blue light, which has a localization depth smaller than that of the SQW emitting green/red light [33]. The temperature dependence of the PL linewidth was fitted using the formula [39]

$$\Gamma = \Gamma_0 + \gamma_{ac} T + \frac{\gamma_{op}}{e^{\hbar\omega_{LO}/k_B T} - 1}, \tag{4}$$

where Γ_0 is the temperature-independent component of the linewidth and γ_{ac} and γ_{op} are the exciton acoustic-phonon and exciton LO-phonon coupling constants, respectively. The best fitted experimental curve provides the values of $\Gamma_0 = 93$ meV, $\gamma_{ac} = 130$ μeV/K, and $\gamma_{op} = 129$ meV, where the LO-phonon energy of $In_{0.92}Al_{0.08}N$ is assumed as $\hbar\omega_{LO} = 76$ meV, with a linear interpolation between the values of InN and AlN. The obtained γ_{ac} value is larger than those reported for GaN (28 μeV/K) and AlN (57 μeV/K) [25], which indicates the dominance of acoustic phonon scattering in linewidth broadening with increasing temperature, or the linear temperature dependence similar to that observed for InN epilayers with relatively low carrier densities ($0.4-2.7 \times 10^{18}$ cm^{-3}) [40].

4 Conclusion We have performed LT-PL measurements of In-rich InAlN NCs grown on Si(111) by rf-MBE. Strong PL intensities were observed in the wavelength range from 0.89 μm to 1.79 μm at 4 K ($0.71 \le x_{In} \le 1.00$), which covers the whole optical communication wavelength range. The temperature dependent emission shift of PL intensity was evaluated for $In_{0.92}Al_{0.08}N$ NCs grown at 480 °C. The PL peak energy shift, known as the "S-shape" PL peak energy shift, was observed with increasing measurement temperature, indicating carrier localization attributed to indium segregation. There was no anomalous blue shift often observed in InN films and nanowires with high residual carrier concentrations. The temperature dependence of PL linewidth was also investigated by using a widely used theoretical model. It was found that acoustic phonon scattering is a dominant factor of the linewidth broadening with increasing temperature.

References

[1] W. M. Yim et al., J. Appl. Phys. **44**, 292 (1972).
[2] Y. Nanishi et al., Jpn. J. Appl. Phys. **42**, 2549 (2003).
[3] J. Wu et al., Appl. Phys. Lett. **80**, 3967 (2002).
[4] X. Wang et al., Jpn. J. Appl. Phys. **45**, L730 (2006).
[5] J.-F. Carlin et al., Phys. Status Solidi B **242**, 2326 (2005).
[6] T. Peng et al., Appl. Phys. Lett. **71**, 2439 (1997).
[7] Q. Guo et al., Jpn. J. Appl. Phys. **42**, L141 (2003).
[8] W. Terashima et al., Jpn. J. Appl. Phys. **45**, L539 (2006).
[9] T. Matsuoka, Appl. Phys. Lett. **71**, 105 (1997).
[10] A. Koukitu et al., Jpn. J. Appl. Phys. **35**, L1638 (1996).
[11] M. Yoshizawa et al., Jpn. J. Appl. Phys. **36**, L459 (1997).
[12] H. Sekiguchi et al., J. Cryst. Growth **300**, 259 (2007).
[13] T. Seppanen et al., J. Appl. Phys. **97**, 083503 (2005).
[14] S.-L. Sahonta et al., Appl. Phys. Lett. **95**, 021913 (2009).
[15] J. Kamimura et al., J. Cryst. Growth **300**, 160 (2007).
[16] I. Vurgaftman et al., J. Appl. Phys. **94**, 3675 (2003).
[17] J. Wu et al., Solid State Commun. **127**, 411 (2003).
[18] R. E. Jones et al., J. Appl. Phys. **104**, 123501 (2008).
[19] B. T. Liou et al., Appl. Phys. A **81**, 651 (2005).
[20] Z. Dridi et al., Semicond. Sci. Technol. **18**, 850 (2003).
[21] R. Goldhahn et al., Phys. Status Solidi A **203**, 42 (2006).
[22] Y. Houchin et al., Phys. Status Solidi C **5**, 1571 (2008).
[23] T. Onuma et al., J. Appl. Phys. **94**, 2449 (2003).
[24] S. Yamaguchi et al., Appl. Phys. Lett. **76**, 876 (2000).
[25] K. B. Nam et al., Appl. Phys. Lett. **85**, 3489 (2004).
[26] R. Zimmermann, J. Cryst. Growth **101**, 346 (1990).
[27] S. M. Lee et al., J. Appl. Phys. **73**, 1788 (1993).
[28] Y. Kawakami et al., Phys. Rev. B **50**, 14655 (1994).
[29] N. Nepal et al., Appl. Phys. Lett. **88**, 062103 (2006).
[30] K. Goodman et al., J. Appl. Phys. **109**, 084336 (2011).
[31] F. B. Naranjo et al., Appl. Phys. Lett. **80**, 231 (2002).
[32] Y. H. Cho et al., Appl. Phys. Lett. **73**, 1370 (1998).
[33] R. Pecharromán-Gallego et al., J. Phys. D **37**, 2954 (2004).
[34] J. Wu et al., Appl. Phys. Lett. **80**, 4741 (2002).
[35] Y. P. Varshni, Physica **34**, 149 (1967).
[36] J. Wu et al., J. Appl. Phys. **94**, 4457 (2003).
[37] C.-H. Shen et al., Appl. Phys. Lett. **88**, 253104 (2006).
[38] P. C. Wei et al., Opt. Express **17**, 11690 (2009).
[39] J. Lee et al., Phys. Rev. B **33**, 5512 (1986).
[40] F. Chen et al., Physica E **20**, 308 (2004).